

PowerFlow-DNN: Compiler-Directed Fine-Grained Power Orchestration for End-to-End Edge AI Inference

Paul Chen, Jeongeun Kim, Wenbo Zhu, Yuanhan Li, Shunyao Huang, Chenjie Weng, and Christopher Torng

Department of Electrical and Computer Engineering
University of Southern California
Los Angeles, CA, USA

Abstract

Edge AI systems often operate under stringent energy and volume constraints that demand extreme efficiency under limited battery capacity, with requirements worsening as intelligent capability demands advance. Prior literature suggests that fine-grained power orchestration, including DVFS and power gating, enables significant energy efficiency benefits that cannot be left unexploited, while still exhibiting unexplored challenges. We observe that layer-level approaches incur unintended overheads due to inter-layer coupling of power control decisions, and that jointly managing these mechanisms under practical constraints such as limited voltage rails and transition overheads leads to a rapidly growing combinatorial schedule space. To address this, we propose PowerFlow-DNN, a compiler-directed framework for end-to-end power-state orchestration in ultra-low-power accelerators. By constructing a rigorous problem formulation for deadline-constrained, real-time, periodic inference as a unified inter-layer power-scheduling problem, our framework enables automated discovery of energy-minimal power-state schedules that adhere to a deadline while accounting for end-to-end, inter-layer impacts. We evaluate the framework on a DNN accelerator VLSI implementation in TSMC 40nm technology. Across representative edge networks, we show that PowerFlow-DNN discovers near-optimal solutions under the discretized formulation and achieves energy within 0.68% of the exact ILP oracle, reducing energy by up to 37% compared to an aggressive baseline without power orchestration, while reasoning over a combinatorial schedule space of over 10^{160} possible power-state assignments, yet operating on a structured layered state graph that enables efficient optimization, achieving up to $2.14\times$ solver speedup via lightweight pruning.

1 Introduction

Edge AI systems increasingly deploy DNN accelerators for local inference under extreme energy and volume constraints, making energy efficiency a primary design challenge due to limited battery capacities, and restricting the complexity of power delivery and voltage regulation infrastructure available on-chip [1, 6, 18, 28, 31].

Dynamic voltage and frequency scaling (DVFS) and power gating are widely used to improve energy efficiency in processors and accelerators [8, 20]. Most prior work assumes coarse-grained global scaling with reactive run-time control, while more recent literature also explores fine-grained scaling and gating with static, compiler-directed control [24, 34]. In this work, we focus on a class of *deadline-constrained, real-time, periodic inference* in embedded AI workloads that, for example, run inference at a fixed frame rate. This captures a limited but relevant subclass of edge AI with the necessary determinism to replace expensive, predictive,

or reactive dynamic power-control overheads with efficient, static, compile-time optimization in futuristic edge AI systems (e.g., smart ingestible capsules [1]).

Determining how to operate fine-grained power-control mechanisms jointly under practical constraints (e.g., transition overheads, limited voltage rails) remains a challenging systems-level problem. Prior work has demonstrated that the energy reduction benefits available through finer-grained power control overcome the energy overheads of the control circuitry, whether supplied through on-chip voltage regulation [19, 29] or multi-rail power supplies [22]. As the computational efficiency demands of edge AI grow, and as researchers study the deployment of ever-smaller power domains to the macro and processing element levels [24, 33] to capture efficiency, the power orchestration schedule space grows combinatorially with the number of power domains, voltage levels, and time interval granularity.

In this work, we make two key observations about the role of fine-grained power orchestration in future edge AI systems. First, we observe that a full, system-level, inter-layer power schedule approach over a DNN execution exposes a *higher ceiling of achievable energy efficiency* than an isolated, layer-by-layer approach due to inherent inter-layer coupling of power control decisions. Second, we observe that building compiler-directed power orchestration can *enable automated solvers to mitigate the challenges of scale* but requires the field to construct problem formulations that capture low-power VLSI implementation details (e.g., energy and transition time overheads, dynamic energy versus static leakage) so that compiler advances can capture energy-delay tradeoffs.

To address this challenge, we propose PowerFlow-DNN (PowerFlow), a compiler-directed framework for power-state orchestration in ultra-low-power DNN accelerators. We formulate DNN inference as an inter-layer power-state scheduling problem that seeks the minimum-energy execution under a real-time deadline constraint. The challenge is not simply selecting lower voltages, but identifying that scheduled decisions at one layer impact or restrict trade-offs in the next layer (e.g., transition time, transition energy across different pairs of voltage rails), thereby producing a minimum-energy sequence of power states under the rail and transition constraints.

The compiler operates on a problem formulation that unifies power gating and DVFS, allowing DVFS compute islands to transition at layer boundaries (natural scheduling points), while producing power-gating schedules for power islands with high-leakage circuitry. Finally, we show that fine-grained power orchestration decisions made by PowerFlow align well with known art and expert intuition based on the law of equi-marginal utility [3, 34] governing the fundamental policy-level tradeoff between energy (utility) and

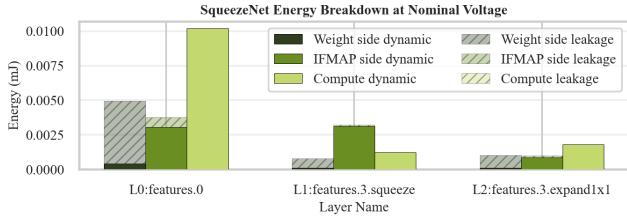


Figure 1: Estimated static and dynamic energy breakdown in TSMC 40 nm for the first three layers of SqueezeNet. The characteristics of these example layers show different needs in space (as seen in the different bars in the cluster), levels (power gating and DVFS), and time (across the three layers).

delay (cost), while allowing the compiler to solve for the detailed schedules itself. Our results show that PowerFlow can automatically discover near-optimal schedules that achieve energy within 0.68% of the exact oracle obtained via ILP (used as the reference solver for small instances), reducing energy by up to 37% compared to an aggressive baseline without power orchestration and achieving up to $2.14\times$ speedup via lightweight pruning. Our domain-aware heuristic pruning approach scales to spaces exceeding 10^{160} , enabling efficient exploration of more complex models and architectures.

Our work also includes two future-looking aspects that do not change the conclusions of the work but highlight applicability: first, emerging non-volatile memories, specifically resistive RAM (RRAM), with bitcell densities to help store ML models entirely in on-chip memory bank arrays in lieu of frequent wireless communication for autonomous edge AI [27]; second, application-level constraints inspired by a biomedical perspective (e.g., smart ingestible capsules [1]), a field demanding both extreme efficiency and intelligence in small form factors. Our contributions are:

- We present evidence that a system-level power scheduling approach can expose a higher ceiling for achievable energy efficiency than traditional layer-by-layer approaches, due to inter-layer coupling in power control decisions.
- We construct a problem formulation for a class of deadline-constrained, real-time, periodic DNN inference that incorporates fine-grained, low-power VLSI techniques and capabilities, sufficient to enable compiler direction and automated solvers for minimizing energy, mitigating the challenges of scale in fine-grained power orchestration.
- We evaluate a compiler-directed power orchestration framework across representative DNN workloads on a vertically integrated toolchain spanning the compiler, architecture, and VLSI implementation in a 40nm technology.

To the best of our knowledge, we are the first to propose a unified problem formulation that jointly optimizes fine-grained DVFS and power gating under realistic VLSI constraints for deterministic edge AI inference workloads to automatically generate cycle-accurate, energy-optimized schedules. We hope that our studies lay the groundwork for future edge AI systems to realize the benefits of fine-grained power orchestration at large scale via automated compiler guidance.

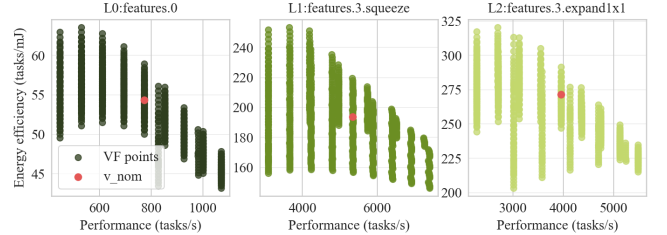


Figure 2: Energy-performance scatter for three SqueezeNet layers under independent DVFS of the compute, RRAM, and feeder domains from any combination of 0.9V to 1.2V; the red marker indicates the nominal operating point. See Section 5 for post-layout level methodology and scaling.

2 Limitations of Conventional DVFS in Edge AI Accelerators

To understand the limitations of conventional DVFS policies in edge AI, we first examine the energy behavior of representative layers and the constraints imposed by emerging memory technologies.

2.1 Energy Composition Varies Across Layers

As the intelligence of bio-integrated devices has increased, the capacity of on-chip memories required to store DNN models and intermediate activations has also grown. Many accelerators, therefore, adopt hybrid memory designs that combine SRAM with emerging non-volatile memories such as RRAM or MRAM to reduce long-term leakage [25–27], but focus on local energy reduction rather than coordinated system-level orchestration across layers.

Emerging memory macros often operate at lower maximum frequencies and exhibit higher access latency than compute logic [23, 26, 27]. Even with data reuse and buffering, memory access and leakage energy remain significant contributors. As a result, the dominant energy source can vary across layers depending on compute intensity, data reuse, and memory access patterns. This variability leads to different optimal operating states across layers, as illustrated in Figure 1. In the remainder of this paper, we use RRAM as a representative emerging memory technology.

2.2 Limitations of Latency-Balanced DVFS

DVFS is a widely used technique for improving energy efficiency in computing systems [7, 8, 13, 17, 34, 37, 39]. Recent works have explored predictive and adaptive DVFS policies for hardware accelerators and heterogeneous systems [8, 20], but do not capture inter-layer dependencies introduced by shared voltage rails.

In contrast to general-purpose processors, bio-integrated accelerators typically execute deterministic inference workloads with fixed computation graphs [1, 28, 32]. In such settings, run-time DVFS policies introduce unnecessary control complexity and may fail to exploit the layer-level variability in energy composition.

Because the energy composition varies significantly across layers, as shown in Figure 1, a fixed global voltage or a latency-balanced DVFS policy can result in suboptimal energy consumption.

Figure 2 illustrates the energy-latency trade-offs obtained by sweeping the voltages of compute and memory domains for several representative layers. The minimum-energy operating point varies across layers and deadlines with different voltage combinations,

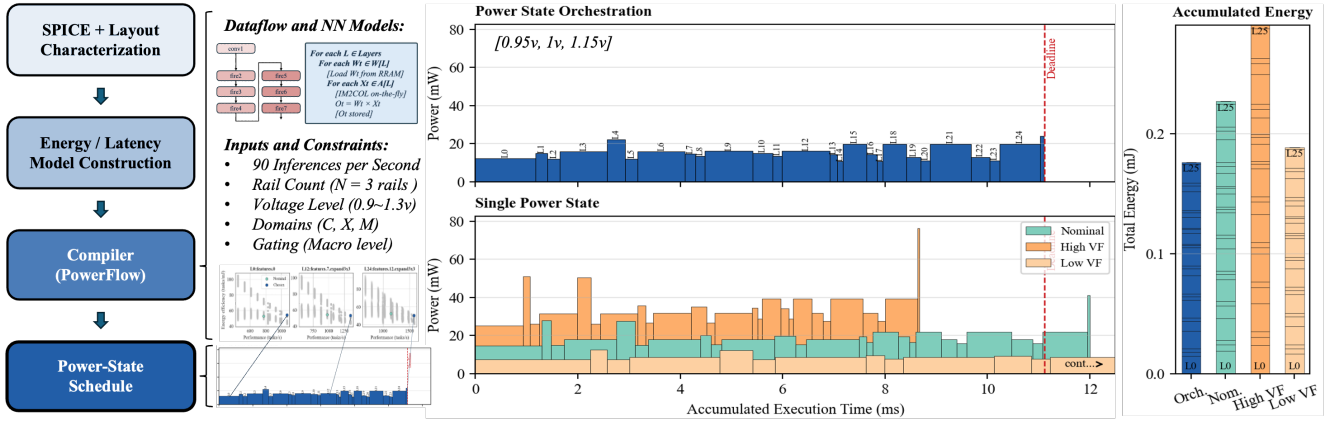


Figure 3: PowerFlow orchestration workflow. The compiler analyzes dataflow and constraints to derive candidate power states per layer (left), then jointly schedules them across layers to meet the inference deadline while minimizing energy (right).

indicating that a single global DVFS policy cannot capture the true energy-optimal schedules under deadline and rail constraints.

2.3 Impact of Rail Scarcity Constraint

While fine-grained voltage scaling has been explored in modern systems [11, 20, 22, 32, 33, 35], practical designs often expose limited supply rails due to power-delivery and integration constraints. This is particularly evident in extreme-edge platforms such as biomedical devices [1, 2, 18], where form-factor limitations limit voltage regulation. As a result, voltage levels must be shared across multiple domains rather than independently controlled. This shared-rail constraint prevents fully independent scaling of compute, memory, and data-movement domains, introducing a system-level challenge: selecting and coordinating a small set of voltage rails across layers while accounting for transition overheads.

2.4 Granularity vs Orchestration Trade-off

Increasing the granularity of power control—through additional voltage rails or independent power domains—enables more precise matching between hardware resources and workload demands. However, this flexibility also exponentially expands the orchestration design space. As the number of layers, domains, and levels increases, the design space grows combinatorially. Consequently, naive heuristics or manual tuning become ineffective, motivating structured optimization to efficiently explore this space.

These observations reveal a fundamental tension: increasing the granularity of power control enables closer approximation to the minimum-energy operating point, but simultaneously expands the orchestration design space beyond what manual tuning or simple heuristics can efficiently explore. This trade-off implies that increasing hardware flexibility alone is insufficient; effective energy minimization requires coordinated power state orchestration across layers. Recent work has explored inter-layer and spatial orchestration in accelerators and reconfigurable architectures [4, 9, 10, 12, 30, 32, 33]. While these approaches coordinate computation and mapping across layers, space, and time, they do not explicitly address power management as a unified optimization problem across DVFS, power gating, and voltage-rail constraints.

3 Architecture and Framework Overview

PowerFlow targets accelerators composed of multiple voltage domains that share limited supply rails. Figure 3 shows the overall orchestration workflow.

3.1 Target Architecture Model

We model the accelerator as a set of controllable power-managed units $D = \{D_1, \dots, D_K\}$, where each unit may correspond to a coarse DVFS-controlled domain or a finer-grained gated memory unit. In our target architecture, these units include coarse DVFS domains (e.g., compute, feeder, and the RRAM memory subsystem) as well as finer-grained memory units, such as independently power-gated memory banks. Each unit operates either at a selected voltage rail or in an active/gated state, depending on its control granularity. Inference executes as a sequence of operations derived from the neural-network dataflow graph. In our prototype system, these operations correspond to neural-network layers, although the formulation applies more generally to any sequence of computational phases. Although our evaluation focuses on a systolic-array accelerator with SRAM buffers and RRAM-based weight storage, the framework applies to any accelerator that exposes multiple voltage domains and power-gating capabilities.

3.2 Power-State Abstraction

Power management decisions in the accelerator consist of two mechanisms: voltage scaling and power gating. This abstraction unifies DVFS and power gating under a single optimization framework. As a result, trade-offs between reducing dynamic energy (via DVFS) and leakage (via gating) can be evaluated jointly, enabling globally optimal scheduling decisions. Both mechanisms are modeled as power-state scheduling decisions. For operation i , a valid operating state specifies the voltage assignments of DVFS-controlled units and the gating schedules of memory-controlled units. These operating states are later formalized as decision variables in the optimization problem.

3.3 Scheduling Anchors

Scheduling decisions occur at execution boundaries (anchors). Layer boundaries provide natural coarse-grained anchors because each layer exhibits stable computation and memory characteristics. Voltages assigned at layer boundaries avoid the overheads of frequent intra-layer rail switching. At finer granularity, memory-access phases provide additional anchors for gating. In particular, banks store weights whose access patterns are determined by the layer dataflow. During portions of execution where a bank’s weights are not required, the bank remains idle and can be temporarily gated to reduce leakage. The compiler identifies such opportunities by analyzing the dataflow graph and the resulting weight-access patterns across execution phases. Consequently, PowerFlow performs inter-layer scheduling of voltage assignments while allowing intra-layer memory gating decisions derived from compiler analysis.

3.4 Compiler Workflow

Compilation occurs once per deployment. The compiler first analyzes the workload dataflow graph to determine memory occupancy, data movement, and domain activity across phases, producing a set of feasible operating points for each operation, each with a distinct combination of power states. Given these candidates, PowerFlow determines the optimal schedule to minimize energy while meeting the target inference deadline with the selected rail constraints, shown in Figure 3. The resulting voltage assignments and memory-gating decisions are compiled into static schedule tables used during run-time execution.

4 Problem Formulation

Based on the architecture model and compiler, we formulate power-state orchestration as a constrained optimization problem.

4.1 System Model

A neural network inference consists of L sequential operations (layers). The accelerator operates on a subset of available voltage rails $\mathcal{R} \subseteq \mathcal{V}$, where \mathcal{V} denotes the discretized set of candidate voltage levels. For each layer i , the solver selects a state $s_i \in \mathcal{S}_i(\mathcal{R})$, where each state specifies a domain-wise assignment $\{V_i^{D_0}, \dots, V_i^{D_K}\}$, with $V_i^{D_k} \in \mathcal{R} \cup \{0\}$ and 0 denoting a gated state. The set $\mathcal{S}_i(\mathcal{R})$ contains all valid operating points for layer i under \mathcal{R} . Each state s_i is characterized by an execution latency $T_{\text{op}}(s_i)$ and an energy $E_{\text{op}}(s_i)$, capturing both static and dynamic components.

Switching between consecutive states incurs latency and energy overhead, captured by transition functions $T_{\text{trans}}(s_{i-1}, s_i)$ and $E_{\text{trans}}(s_{i-1}, s_i)$. Transitions are assumed not to overlap with computation. The accelerator supports at most N_{max} voltage rails. For deterministic edge inference workloads, the inference deadline is a fixed scalar: $T_{\text{max}} = 1/R_{\text{target}}$. For completeness, we include a terminal state s_{L+1} to model the idle interval before T_{max} .

4.2 Optimization Objective

The continuous voltage range $[V_{\text{min}}, V_{\text{max}}]$ is discretized into a finite candidate set \mathcal{V} using a uniform step size ΔV . The optimization selects a rail subset $\mathcal{R} = \{V_1, \dots, V_N\}$, where $V_n \in \mathcal{V}$ and $|\mathcal{R}| \leq N_{\text{max}}$, and selects a sequence of states $s_i \in \mathcal{S}_i(\mathcal{R})$.

Total inference time is

$$T_{\text{infer}} = \sum_{i=1}^L T_{\text{op}}(s_i) + \sum_{i=1}^L T_{\text{trans}}(s_i, s_{i+1}) \quad (1)$$

where transition overheads capture rail-switching and memory wake events. We formulate cross-layer power-state orchestration as the following optimization:

$$\min_{\mathcal{R}, s_1, \dots, s_L, s_{L+1}} E_{\text{tot}} = \sum_{i=1}^L E_{\text{op}}(s_i) + \sum_{i=1}^L E_{\text{trans}}(s_i, s_{i+1}) + E_{\text{idle}}(s_{L+1}) \quad (2)$$

subject to

$$|\mathcal{R}| \leq N_{\text{max}}, \mathcal{R} \subseteq \mathcal{V}, T_{\text{infer}} \leq T_{\text{max}}, s_i \in \mathcal{S}_i(\mathcal{R}), i = 1, \dots, L.$$

The terminal state s_{L+1} models the idle interval following the final transition. Let $z \in \{0, 1\}$ denote the duty-cycling decision, where $z = 1$ indicates that the accelerator remains active during the idle interval. The idle energy is given by $E_{\text{idle}}(s_{L+1}) = z \cdot P_{\text{idle}} \cdot [T_{\text{max}} - T_{\text{infer}}]$, where P_{idle} denotes the idle power, capturing both static leakage and residual dynamic power under clock gating. Thus, idle energy is incurred only when the accelerator remains active.

We note that the configuration energy associated with programming control registers is not included, as it is a one-time cost offset not controlled by the solver and independent of the selected schedule. The voltage–frequency relation is implicitly captured in the latency and energy of each s_i , and the resulting search space grows combinatorially with the number of rail subsets, layers, domains, and voltage levels, making exhaustive search intractable.

Unlike prior work that assumes constant or linear transition costs, we model transition energy and latency as pairwise functions between states, capturing asymmetric and domain-dependent switching behavior. While our evaluation uses a simplified transition model, the formulation generalizes to detailed, characterization-driven transition costs without modification. This formulation highlights that operating states are coupled across layers due to shared rails and transition overheads.

From the defined optimization function, the full schedule space is upper-bounded by $\sum_{k=1}^{N_{\text{max}}} \binom{|\mathcal{V}|}{k} (k+1)^{DL}$, which grows exponentially in the number of layers and domains. While this defines a worst-case combinatorial schedule space, the DP-based algorithm instead operates on a layered state graph of feasible per-layer states. The effective complexity therefore depends on the number of states across layers, $\sum_{i=1}^{L+1} |\mathcal{S}_i|$, and the transitions between adjacent layers, $\sum_{i=1}^L |\mathcal{S}_i| |\mathcal{S}_{i+1}|$, rather than the full schedule space.

4.3 Solution Approach

While ILP provides the exact solution for the constrained formulation, it becomes impractical for large full-network instances due to combinatorial growth in the scheduling space. Consequently, we rely on a dynamic-programming (DP) algorithm for scalable optimization. We use ILP formulations only for validation on small instances.

For each operation, the framework enumerates feasible operating states together with their latency and energy, as described in Section 3.4. Because transitions incur latency and energy overhead, the problem cannot be decomposed into independent per-layer decisions. PowerFlow therefore models scheduling as a shortest-path

Table 1: Accelerator hardware configuration.

Category	Configuration
Technology	TSMC 40 nm
Compute/Memory System	
Architecture	Output-stationary
Dataflow	Weight tile reuse
Systolic Array Size	8 × 8 PEs
MAC Precision	INT8
RRAM Weight Storage	Model Dependent
Activation Scratchpad	Model Dependent
Lane Buffers	72 × 8 entries (ping-pong)
Weight Buffer	576 × 8 entries (ping-pong)

problem over a layered state graph under rail constraints. To meet the inference deadline, we solve this using a Lagrangian formulation and a DP-based search (referred to as λ -DP), where λ controls the energy–latency tradeoff by reweighting the objective as $E + \lambda T$. For each fixed λ , the DP algorithm computes the exact optimum of the weighted objective. By performing a parametric search over λ , we identify feasible solutions under the latency constraint. While the weighted formulation may, in principle, miss unsupported optima in discrete settings, the DP algorithm remains exact for each weighted subproblem and efficiently identifies high-quality feasible solutions in practice. Algorithm scalability and validation are evaluated in Section 6.5.

4.4 Solver Variants

Traditional solvers have well-known scalability limits. We consider adding *domain-specific, heuristic extensions* to the solver to improve solver efficiency and mitigate limitations as the combinatorial space grows, without modifying the underlying optimization or final quality of results. Our specific techniques have mixed results but set the stage for future domain-specific heuristics to improve upon solver efficiency. The unoptimized solver operates on the full candidate state space and performs a Lagrangian search starting from $\lambda = 0$, increasing λ until a feasible schedule is found, followed by binary search refinement.

Structure pruning is a heuristic that removes dominated states within each layer. A state s_A is pruned if there exists another state s_B whose voltage set is a subset of that of s_A , and that is no worse in energy, run time, or leakage, with at least one strict improvement. This removes Pareto-dominated points while preserving the set of high-quality candidates, reducing the effective state space.

Marginal-utility jump heuristic builds on structure pruning by using path-aware marginal tradeoffs to guide the λ search. Starting from $\lambda = 0$, if the resulting schedule is infeasible, the solver greedily applies single-layer upgrades that maximize marginal utility, accounting for both per-layer and transition costs. These upgrades define candidate crossover λ values, which are used as jump points before continuing standard bracketing and binary search.

The heuristic is a localized, discrete approximation of the law of equi-marginal utility, but because our problem operates over a discretized schedule space with non-convex transition costs and shared rail constraints, our results in Section 6.6 show that these local trade-offs do not consistently improve solution quality or search efficiency.

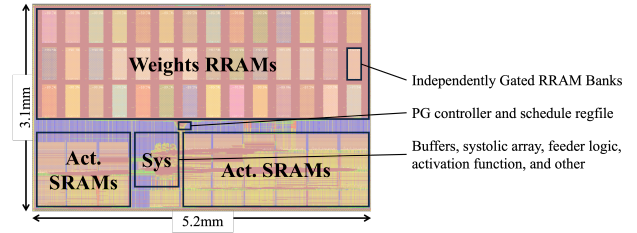


Figure 4: 40 nm accelerator layout used for calibration. The chip operates up to 500 MHz, with the RRAM subsystem at 100 MHz. RRAM banks are power-gated at the macro level, while higher-level domain control is modeled architecturally.

Table 2: Workload Characteristics

Model	Layers	Layer Types
SqueezeNet1.1 [16]	26	Conv, Fire
MobileNetV3-Small [15]	52	DW, Conv, SE
ResNet18 [14]	20	Conv, Residual
MobileViT-xxs [21]	72	Conv, Attention

5 Evaluation Methodology

To study the proposed co-optimization problem, we model the accelerator subsystem, including DVFS and duty-cycling mechanisms, under a limited rail-count constraint.

5.1 Hardware and Modeling Setup

power-domain implementation. Table 1 summarizes our evaluation parameters. A representative accelerator instance (configured for SqueezeNet) is fully synthesized and place-and-routed in TSMC 40 nm LP technology, shown in Figure 4, to obtain post-layout timing, area, and energy for characterization, enabling our study on system-level orchestration.

RRAM bank activity is determined from the deterministic weight-address stream generated by the DMA engine, which reflects the accelerator’s dataflow schedule. These events serve as scheduling anchors as mentioned in section 3.3. The run-time follows the compiler-generated schedule without additional control logic.

Energy consumption is obtained from post-synthesis gate-level power analysis and used to construct a per-event energy lookup model capturing compute, memory, and data-movement events. SRAM access energy and leakage are extracted from the TSMC memory compiler, while RRAM characteristics follow prior work [26, 27]. All workloads use INT8 precision for both weights and activations.

A cycle-accurate performance model is used to estimate layer latency and generate activity counts for the energy model, validated against RTL simulations. Candidate schedules are validated against post-layout timing limits obtained from static timing analysis at the typical PVT corner. In practice, the target PVT corner should match the specific deployment environment, ensuring that the schedules remain timing-safe under real-world operating conditions.

5.2 DVFS and Transition Modeling

Voltage-frequency scaling is derived from SPICE characterization of an FO4-loaded ring oscillator in the target 40 nm LP process. Energy scaling follows a first-order voltage–frequency model [33]. Voltages range from 0.9–1.3 V (step 0.05).

We assume schedule updates are prepared in parallel via shadow configuration registers at scheduling boundaries. As a result, configuration latency is treated as a one-time offset and is not modeled as part of the execution or transition latency.

Switching between supply rails incurs latency, energy, and area overhead due to charging and discharging the domain capacitance through the power-switch network. Consistent with prior studies [36, 38], we assume worst-case transition latencies from circuit-level modeling: 5 ns for memory wake-up and 15 ns for DVFS rail switching. Transition energy is modeled as $E_{switch} = C_{dom}(V_{high}^2 - V_{low}^2)$. We assume a nominal transition energy of 1 nJ and evaluate sensitivity over 0.1 nJ–1 μ J. While level shifter overheads between voltage domains are not explicitly modeled, their impact is small relative to memory and compute energy, and can be incorporated into the transition cost model without changing the formulation.

We capture area overhead at the chip level, including the centralized *pg_manager* and three clock-generation blocks, which contribute 0.24% of total area. For larger domain schedules, domain-level overhead is extrapolated from per-macro measurements, resulting in 4.6–9.2% area across domains depending on domain size.

5.3 Workloads and Metrics

Table 2 summarizes the evaluated workloads, including diverse layer types (conv, depthwise, residual, attention), leading to different dataflows and power-management opportunities across layers.

Energy is reported per interval in the continuous inference setting, where idle periods between inferences depend on the target inference rate and the balance between static and dynamic energy.

6 Evaluation

We evaluate whether PowerFlow identifies the minimum-energy operating point under discretized voltage and power-state spaces, and compare against strong heuristic baselines. Specifically, we examine: (1) energy reduction across inference rates compared to baseline policies, (2) generalization across representative networks, (3) the impact of hardware constraints, and (4) solver scalability.

The baseline corresponds to a conventional accelerator design without cross-layer power optimization [5]. The +gating variant extends this design with fine-grained memory power gating inspired by prior work [26, 27]. The +greedy policy applies a layer-wise DVFS heuristic that selects locally optimal operating points under latency constraints, consistent with prior approaches [8, 20, 33]. We define layer-wise DVFS as a greedy marginal-utility-based policy that iteratively adjusts per-layer voltage assignments to meet a global deadline, without accounting for inter-layer transition costs. We compare these baselines, their combination, and the proposed PowerFlow under identical hardware and timing constraints.

6.1 Energy vs Inference Rate

Figure 5 shows energy per inference interval sweeping the target inference rate. Fine-grained power gating significantly reduces energy by eliminating leakage from idle RRAM banks. In contrast, greedy DVFS alone focuses on dynamic energy, not static energy nor inter-layer transition costs. Combining DVFS and power gating improves energy efficiency and is sufficient at lower inference rates where slack is abundant. However, it remains suboptimal at higher

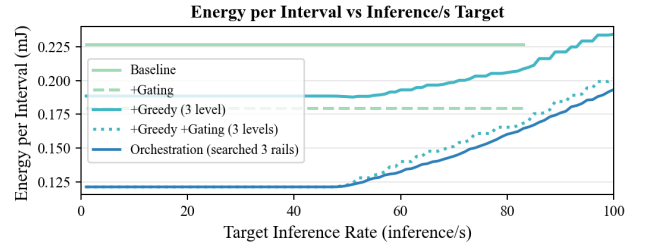


Figure 5: Energy per inference interval versus target inference rate for SqueezeNet. We compare baseline, +gating, +greedy, +gating+greedy and the proposed orchestration with optimized rail selection (see Section 6 for definitions).

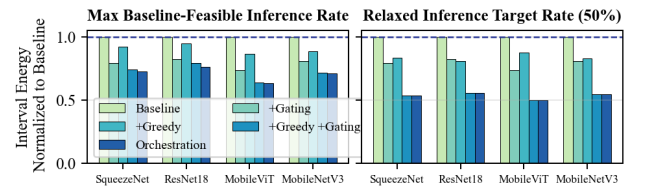


Figure 6: Normalized energy per inference across four edge models under tight and relaxed deadlines.

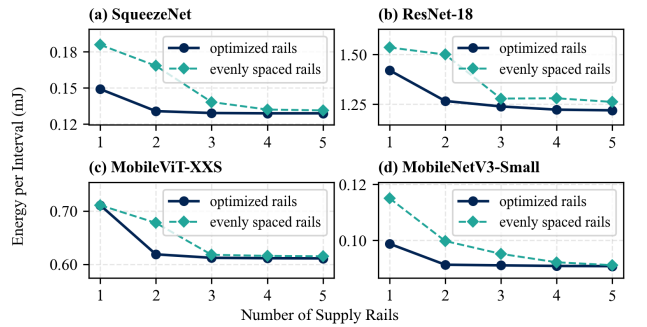


Figure 7: Energy per inference vs. available voltage rail count. We compare evenly spaced rails and optimized rails, both evaluated under the PowerFlow orchestration.

rates due to locally optimized decisions. PowerFlow achieves lower energy by jointly optimizing voltage rail selection and power-state schedules while accounting for transition overheads.

6.2 Generalization Across Models

To evaluate generality, we repeat the experiment across four representative edge networks, shown in Figure 6. At each model’s maximum feasible inference rate, PowerFlow reduces energy by 25–37% compared to the unoptimized baseline and achieves an additional 2–7% reduction relative to the +greedy+gating baseline. Under relaxed deadlines, PowerFlow and the +greedy+gating baseline achieve similar energy levels, as abundant slack allows layers to operate near their minimum-energy points, limiting the benefit of cross-layer orchestration.

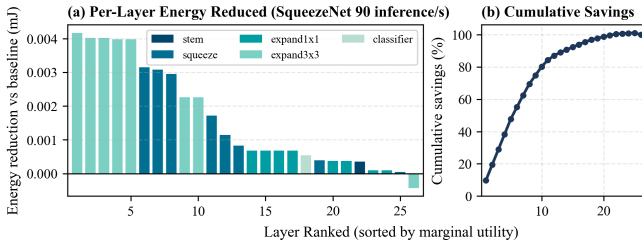


Figure 8: Layers are sorted by local marginal utility, defined as energy reduction per unit latency increase from the nominal operating point. Bars show per-layer energy reduction for the compiler output schedule as Figure 3.

6.3 Impact of Voltage Rail Availability

Voltage rail availability directly affects the achievable minimum energy. As shown in Figure 7, increasing the number of rails allows the scheduler to better approximate per-layer optimal operating points. Energy decreases by 7–14% when increasing from one to three rails, with diminishing returns beyond three rails. Additionally, optimized rail selection improves efficiency by up to 13% compared to evenly spaced rails when the number of rails is limited. This suggests that a small number of carefully chosen rails captures most of the achievable energy savings, highlighting that rail selection is more impactful than increasing the number of voltage levels.

6.4 Additional Observations

The orchestration framework enables rapid analysis to surface insights into different domain scenarios, voltage-state availability, and the impact of transition latency. **Power-domain granularity:** Separating compute and memory into independent domains extended the range of energy reduction by 11%, while further partitioning provided only marginal additional benefits, indicating diminishing returns beyond coarse domain decoupling. **Memory power-gating granularity:** Enabling fine-grained gating of memory macros resulted in reduced leakage by up to 90%, and both greedy and orchestration remain the same results before the break-even point. This suggests that hardware gating already captures most leakage savings in these regimes. **Transition overhead sensitivity:** We swept transition energy overhead across four orders of magnitude (data omitted for space) and saw that the optimizer naturally reduces switching events when the costs increase. Voltage transitions are only selected when the expected energy savings outweigh the overhead. **Local marginal utility:** Energy savings exhibit a skewed distribution across layers, with the majority contributed by a small subset. In Figure 8, the top ten layers account for approximately 80% of the total achievable energy reduction. Beyond this point, additional layers provide diminishing returns, and low-utility operating states may even increase energy consumption under deadline constraints. This behavior is consistent with the law of equi-marginal utility, where optimal allocation equalizes marginal energy savings per unit latency across layers.

6.5 Solver Scalability

Finally, we evaluate the scalability of the orchestration solver in Figure 9. Run-time scales with the size of the layered state graph rather than the full combinatorial schedule space. The ILP formulation

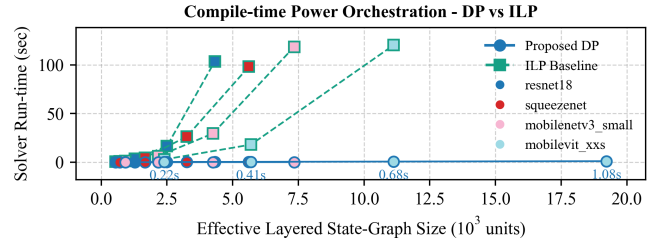


Figure 9: Solver run-time versus explored layered-state graph size (feasible state graph defined in Section 4.2).

scales poorly with the combinatorial schedule space and becomes impractical even with reduced voltage levels. In contrast, the λ -DP algorithm scales efficiently and returns solutions within seconds, enabling exploration of more complex models and architectures. We use **ILP as the oracle** for small instances, and observe that the λ -DP algorithm achieves solutions within 0.68% of optimal under the discretized formulation. While the weighted formulation may, in principle, miss unsupported optima in discrete settings, this effect remains small in practice.

6.6 Solver Variants

We observe that structure pruning produces identical solutions to the unoptimized solver across all evaluated workloads. While pruning is based on local dominance and could, in principle, remove states that are beneficial under certain transition patterns, we do not observe any loss of optimality in our experiments. Structure pruning consistently reduces solver run-time, achieving up to 2.14 \times average speedup over the baseline across inference rates of 1–100 FPS, and 1.31 \times over the more constrained 50–100 FPS regime for SqueezeNet (excluding preprocessing cost). The marginal-utility jump heuristic exhibits mixed behavior and does not consistently improve over pruning alone, suggesting that while marginal utility captures useful local tradeoffs, it is not uniformly effective for guiding λ search. This highlights the challenges of directly applying marginal-utility principles in globally coupled, discrete-optimization settings, where local trade-offs do not always add up to globally optimal schedules.

Across all experiments, PowerFlow consistently identifies near-minimum-energy schedules under realistic rail and domain constraints. The results reveal three key insights: (1) a small number of voltage rails captures most of the achievable energy savings, (2) separating compute and memory domains significantly improves energy efficiency, and (3) optimal orchestration naturally suppresses excessive switching when transition overheads increase.

7 Conclusion

Fine-grained DVFS and power gating are increasingly available in modern AI accelerators, but exploiting this flexibility is challenging in rail-constrained systems with shared voltage domains. Our results show that layer-wise DVFS heuristics fail to capture inter-layer transition costs and shared-rail interactions. By formulating power management as a unified orchestration problem, PowerFlow-DNN identifies energy-efficient schedules that satisfy inference deadlines under realistic constraints. These results demonstrate that fine-grained control alone is insufficient—structured orchestration is required to realize its full potential. Future work includes

exploring workload-aware voltage-rail design and improving solver efficiency through more robust domain-specific search strategies for discrete, globally coupled optimization spaces.

References

- [1] Angsagan Abdigazy, Mohammed Arfan, Gianluca Lazzi, Constantine Sideris, Alex Abramson, and Yasser Khan. 2024. End-to-end design of ingestible electronics. *Nature Electronics* (Feb 2024).
- [2] Angsagan Abdigazy, Mohammed Arfan, June Shao, Mohammad Islam Shafiqul, Md Farhad Hassan, and Yasser Khan. 2024. 3D gas mapping in the gut with AI-enabled ingestible and wearable electronics. *Cell Reports Physical Science* (Jul 2024).
- [3] Omid Azizi, Aqeel Mahesri, Benjamin C. Lee, Sanjay J. Patel, and Mark Horowitz. 2010. Energy-performance Tradeoffs in Processor Architecture and Circuit Design: A Marginal Cost Analysis. *Int'l Symp. on Computer Architecture (ISCA)* (Jun 2010).
- [4] Chen Bai, Xuechao Wei, Youwei Zhuo, Yi Cai, Hongzhong Zheng, Bei Yu, and Yuan Xie. 2024. Klotksi v2: Improved dnn model orchestration framework for dataflow architecture accelerators. *IEEE Trans. on Computer-Aided Design of Integrated Circuits and Systems (TCAD)* (Aug 2024).
- [5] Yu-Hsin Chen, Tushar Krishna, Joel S. Emer, and Vivienne Sze. 2017. Eyeriss: An Energy-Efficient Reconfigurable Accelerator for Deep Convolutional Neural Networks. *IEEE Journal of Solid-State Circuits (JSSC)* (Jan 2017).
- [6] Guy Eichler, Yatin Gilhotra, Nanyu Zeng, Martha Kim, Kenneth Shepard, and Luca Carloni. 2025. MINDFUL: Safe, Implantable, Large-Scale Brain-Computer Interfaces from a System-Level Design Perspective. *Int'l Symp. on Microarchitecture (MICRO)* (Oct 2025).
- [7] Stijin Eyerman and Lieven Eeckhout. 2011. Fine-Grained DVFS Using On-Chip Regulators. *ACM Trans. on Architecture and Code Optimization (TACO)* 8, 1 (Apr 2011), 1:1–1:24.
- [8] Jiawei Geng, Zongwei Zhu, Weihong Liu, Xuehai Zhou, and Boyu Li. 2026. PowerLens: An Adaptive DVFS Framework for Optimizing Energy Efficiency in Deep Neural Networks. *Design Automation Conf. (DAC)* (Jan 2026).
- [9] Graham Gobieski, Ahmet Oguz Atli, Kenneth Mai, Brandon Lucia, and Nathan Beckmann. 2021. Snafu: An Ultra-Low-Power, Energy-Minimal CGRA-Generation Framework and Architecture. *Int'l Symp. on Computer Architecture (ISCA)* (Jun 2021).
- [10] Graham Gobieski, Souradip Ghosh, Marijn Heule, Todd Mowry, Tony Nowatzki, Nathan Beckmann, and Brandon Lucia. 2022. Riptide: A programmable, energy-minimal dataflow compiler and architecture. *Int'l Symp. on Microarchitecture (MICRO)* (Oct 2022).
- [11] Wacław Godycki, Christopher Torng, Ivan Bukreyev, Alyssa Apsel, and Christopher Batten. 2014. Enabling Realistic Fine-Grain Voltage Scaling with Reconfigurable Power Distribution Networks. *Int'l Symp. on Microarchitecture (MICRO)* (Dec 2014).
- [12] Yu Gong, Lingyi Huang, Haodong Chang, Rongjian Liang, Cheng Yang, Zhexiong Tang, Jiang Hu, and Bo Yuan. 2025. Crane: Inter-Layer Scheduling Framework for DNN Inference and Training Co-Support on Tiled Architecture. *Int'l Symp. on Microarchitecture (MICRO)* (Oct 2025).
- [13] Jawad Haj-Yahya, Mohammed Alser, Jeremie Kim, A. Giray Yağlıkçı, Nandita Vijaykumar, Efraim Rotem, and Onur Mutlu. 2020. SysScale: Exploiting Multi-domain Dynamic Voltage and Frequency Scaling for Energy Efficient Mobile Processors. *Int'l Symp. on Computer Architecture (ISCA)* (Jul 2020).
- [14] Kaiming He, Xiangyu Zhang, Shaoqing Ren, and Jian Sun. 2016. Deep residual learning for image recognition. *ICCV* (Jun 2016).
- [15] Andrew Howard, Mark Sandler, Grace Chu, Liang-Chieh Chen, Bo Chen, Mingxing Tan, Weijun Wang, Yukun Zhu, Ruoming Pang, Vijay Vasudevan, et al. 2019. Searching for mobilenetv3. *ICCV* (May 2019).
- [16] Forrest N Iandola, Song Han, Matthew W Moskewicz, Khalid Ashraf, William J Dally, and Kurt Keutzer. 2016. SqueezeNet: AlexNet-level accuracy with 50x fewer parameters and < 0.5 MB model size. *arXiv preprint arXiv:1602.07360* (Nov 2016).
- [17] C. Isci and M. Martonosi. 2006. Live, Runtime Phase Monitoring and Prediction on Real Systems with Application to Dynamic Power Management. *Int'l Symp. on Microarchitecture (MICRO)* (Dec 2006).
- [18] Yaoyao Jia, Ulkuhan Guler, Yen-Pang Lai, Yan Gong, Arthur Weber, Wen Li, and Maysam Ghovanloo. 2021. A Trimodal Wireless Implantable Neural Interface System-on-Chip. *IEEE Transactions on Biomedical Circuits and Systems* (Nov 2021).
- [19] S. S. Kudva and R. Harjani. 2011. Fully-Integrated On-Chip DC-DC Converter With a 450X Output Range. *IEEE Journal of Solid-State Circuits (JSSC)* 46, 8 (Aug 2011), 1940–1951.
- [20] Siqin Liu and Avinash Karanth. 2022. Dynamic Voltage and Frequency Scaling to Improve Energy-Efficiency of Hardware Accelerators. *Int'l Conf. on High-Performance Computing (HIPC)* (Jan 2022).
- [21] Sachin Mehta and Mohammad Rastegari. 2021. Mobilevit: light-weight, general-purpose, and mobile-friendly vision transformer. *arXiv preprint arXiv:2110.02178* (Oct 2021).
- [22] Timothy N. Miller, Xiang Pan, Renji Thomas, Naser Sedaghati, and Radu Teodorescu. 2012. Booster: Reactive Core Acceleration For Mitigating the Effects of Process Variation and Application Imbalance in Low-Voltage Chips. *Int'l Symp. on High-Performance Computer Architecture (HPCA)* (Feb 2012).
- [23] Gabriel Molas and Etienne Nowak. 2021. Advances in Emerging Memory Technologies: From Data Storage to Artificial Intelligence. *Applied Sciences* (Nov 2021).
- [24] Ankita Nayak, Keyi Zhang, Raj Setaluri, Alex Carsello, Makai Mann, Christopher Torng, Stephen Richardson, Rick Bahr, Pat Hanrahan, Mark Horowitz, and Priyanka Raina. 2023. Improving Energy Efficiency of CGRAs with Low-Overhead Fine-Grained Power Domains. *ACM Trans. on Reconfigurable Technology and Systems (TRETS)* (Apr 2023).
- [25] Fabian Oboril, Rajendra Bishnoi, Mojtaba Ebrahimi, and Mehdi B. Tahoori. 2015. Evaluation of Hybrid Memory Technologies Using SOT-MRAM for On-Chip Cache Hierarchy. *IEEE Trans. on Computer-Aided Design of Integrated Circuits and Systems (TCAD)* (Jan 2015).
- [26] Kartik Prabhu, Albert Gural, Zainab F Khan, Robert M Radway, Massimo Giordano, Kalhan Koul, Rohan Doshi, John W Kustin, Timothy Liu, Gregorio B Lopes, et al. 2022. CHIMERA: A 0.92-TOPS, 2.2-TOPS/W edge AI accelerator with 2-MByte on-chip foundry resistive RAM for efficient training and inference. *IEEE Journal of Solid-State Circuits (JSSC)* (Jan 2022).
- [27] Kartik Prabhu, Robert M Radway, Y Jeffrey, Kai Bartolone, Massimo Giordano, Fabian Peddinghaus, Yonatan Urman, Win-San Khwa, Yu-Der Chih, Meng-Fan Chang, et al. 2024. MINOTAUR: An edge transformer inference and training accelerator with 12 MBytes on-chip resistive RAM and fine-grained spatiotemporal power gating. *Symp. on Very Large-Scale Integration Technology and Circuits (VLSI)* (Jun 2024).
- [28] Ali Sahafi, Y Wang, CLM Rasmussen, P Bollen, G Baatrup, V Blanes-Vidal, J Herp, and ES Nadimi. 2022. Edge artificial intelligence wireless video capsule endoscopy. *Scientific Reports* (Aug 2022).
- [29] Michael Seeman. 2009. *A Design Methodology for Switched-Capacitor DC-DC Converters*. Ph.D. Dissertation. EECS Department, University of California, Berkeley.
- [30] Nathan Serafin, Souradip Ghosh, Harsh Desai, Nathan Beckmann, and Brandon Lucia. 2023. Pipestitch: An energy-minimal dataflow architecture with lightweight threads. *Int'l Symp. on Microarchitecture (MICRO)* (Dec 2023).
- [31] Liufang Sheng, Xuanxu Chen, Yuejun Zhang, Ke Yan, Junping Chen, Zhikang Chen, Hanyu Shi, and Yi Gong. 2025. Design of a hybrid AI network circuit for epilepsy detection with 97.5% accuracy and low cost-latency. *Frontiers in Physiology* (Mar 2025).
- [32] Cheng Tan, Miaomiao Jiang, Deepak Patil, Yanghui Ou, Zhaoying Li, Lei Ju, Tulika Mitra, Hyunchul Park, Antonino Tumeo, and Jeff Zhang. 2024. ICED: An Integrated CGRA Framework Enabling DVFS-Aware Acceleration. *Int'l Symp. on Microarchitecture (MICRO)* (Dec 2024).
- [33] Christopher Torng, Peitian Pan, Yanghui Ou, Cheng Tan, and Christopher Batten. 2021. Exploring Coarse-Grained Reconfigurable Architectures for Irregular Loop Specialization using Ultra-Elastic Dataflow. *Int'l Symp. on High-Performance Computer Architecture (HPCA)* (Apr 2021).
- [34] Christopher Torng, Moyang Wang, and Christopher Batten. 2016. Asymmetry-Aware Work-Stealing Runtimes. *Int'l Symp. on Computer Architecture (ISCA)* (Jun 2016).
- [35] D.N. Truong, W.H. Cheng, T. Mohsenin, Zhiyi Yu, A.T. Jacobson, G. Landge, M.J. Meeuwse, C. Watnik, A.T. Tran, Zhibin Xiao, E.W. Work, J.W. Webb, P.V. Mejia, and B.M. Baas. 2009. A 167-Processor Computational Platform in 65-nm CMOS. *IEEE Journal of Solid-State Circuits (JSSC)* 44, 4 (Apr 2009), 1130–1144.
- [36] Kimiyoshi Usami, Toshiaki Shirai, Tasunori Hashida, Hiroki Masuda, Seidai Takeda, Mitsutaka Nakata, Naomi Seki, Hideharu Amano, Mitaro Namiki, Masashi Imai, Masaaki Kondo, and Hiroshi Nakamura. 2009. Design and Implementation of Fine-Grain Power Gating with Ground Bounce Suppression. *Int'l Conf. on VLSI Design (VLSID)* (Jan 2009).
- [37] M. Weiser, B. Welch, A. J. Demers, and S. Shenker. 1994. Scheduling for Reduced CPU Energy. *Symp. on Operating System Design and Implementation (OSDI)* (1994).
- [38] Yuqi Xue and Jian Huang. 2025. ReGate: Enabling Power Gating in Neural Processing Units. *Int'l Symp. on Microarchitecture (MICRO)* (Oct 2025).
- [39] Bo Zhai, David Blaauw, Dennis Sylvester, and Krisztian Flautner. 2005. The Limit of Dynamic Voltage Scaling and Insomniac Dynamic Voltage Scaling. *IEEE Trans. on Very Large-Scale Integration Systems (TVLSI)* (Nov 2005).